Electron transfer between cytochrome c and the binuclear center of cytochrome oxidase.

Mariana Rocha , Roger Springett

PII: S0022-5193(18)30498-3
DOI: https://doi.org/10.1016/j.jtbi.2018.10.022
Reference: YJTBI 9665

To appear in: *Journal of Theoretical Biology*

Received date: 9 July 2018
Revised date: 5 October 2018
Accepted date: 8 October 2018

Please cite this article as: Mariana Rocha , Roger Springett , Electron transfer between cytochrome c and the binuclear center of cytochrome oxidase., *Journal of Theoretical Biology* (2018), doi: https://doi.org/10.1016/j.jtbi.2018.10.022

Highlights

- A simplified *in-silico* kinetic model of Cytochrome Oxidase is developed
- The model includes Cytochrome c binding, oxidation and reduction of oxygen
- It reproduces the experimental reduction of Cu_A, heme *a* and heme a_3 during turnover
- It predicts that the off rate constants for oxidized and reduced Cyt*c* can be unequal
- Disequilibrium between Cyt*c* and Cu_A results in the non-Nernst response of heme *a*

Electron transfer between cytochrome *c* and the binuclear center of cytochrome oxidase.

Mariana Rocha and Roger Springett

Cardiovascular Division, King's College London British Heart Foundation Center of Excellence, London, United Kingdom

Running title: Electron transfer between Cyt*c* and the BNC

Address all correspondence to Roger Springett at:

e-mail: Roger.Springett@kcl.ac.uk

Abstract

The Minnaert model, which can account for the reaction kinetics between cytochrome oxidase and cytochrome *c* (Cyt*c*), has been used to justify equal binding rate constants for reduced and oxidized Cyt*c*. Here we extend the model beyond reversible binding of Cyt*c* and its irreversible oxidation to include Cu_A, heme *a* and the oxidation cycle of the binuclear center. The model reproduces the experimental reduction of Cu_A and heme *a* during turnover and the low population of the ferryl and ferrous heme a_3. It predicts that the off rate constants for reduced and oxidized Cyt*c* can be unequal and that the non-Nernst response of Cu_A and heme *a* is due to disequilibrium between free Cyt*c* and Cu_A rather than redox anticooperativity

Keywords: Cytochrome oxidase, enzyme kinetics, enzyme modeling, midpoint potential, redox anti-cooperativity and proton pumping.

Introduction

Cytochrome aa_3 oxidase (CytOx) is the terminal proton pumping enzyme of the mitochondrial electron transport chain and uses electrons delivered by intermembrane cytochrome c (Cyt*c*) to reduce oxygen to water. Electrons from bound Cyt*c* are first passed to the Cu_A center just beneath the Cyt*c* binding site and then onto heme *a* buried in the complex at a depth of ≈1/3 of the membrane thickness [1]. From there, they are passed parallel to the membrane to the binuclear center (BNC), consisting of heme a_3 and Cu_B, where oxygen is reduced to water using protons from the matrix. Conrad and Smith [2] found that the turnover number was strictly first order with reduced Cyt*c* as reduced Cyt*c* was consumed and oxidized Cyt*c* was produced during catalytic turnover. They also found that CytOx follows Michaelis-Menten kinetics [3] (first proposed by Henri, see [4]) so that the turnover must be given by:

$$v = \frac{k_{cat}[c^{2+}]}{[c^{2+}]+[c^{3+}]+K_M} \qquad \text{Equation 1}$$

where $[c^{2+}]$ and $[c^{3+}]$ are the concentration of reduced and oxidized Cyt*c*, respectively. Later, Minnaert [5] developed a model where both oxidized and reduced Cyt*c* can reversibly bind to CytOx, and the bound reduced Cyt*c* is oxidized by the downstream oxygen reaction (fig. 1a). This model can account for the so-called Smith-Conrad kinetics of eqn. 1 if (1) the binding rate constants of reduced and oxidized Cyt*c* are the same and (2) the oxidation of bound Cyt*c* is unidirectional (irreversible). Since the midpoint potentials of Cyt*c* and Cu_A are similar (260 [6] and 250mV [7], respectively) and the rate constants for electron transfer are large (>100,000s^{-1} [8]), the Cu_A center would have to be held in a fully oxidized state by the oxygen reaction at the BNC in order to ensure unidirectional electron transfer between bound Cyt*c* and the Cu_A center. Interestingly, the recent measurement of the Cu_A and heme *a* oxidation states simultaneously with turnover [6] have shown that both Cu_A and heme *a* are considerably reduced at high turnover. This lead to the presumption that Cyt*c*, Cu_A and heme *a* remain in close equilibrium, contrary to the requirements of the Minnaert model. However the reduction state of the centers did not follow a simple n=1 Nernst function and it was concluded that there must be considerable redox anti-cooperativity between Cu_A, heme *a* and Cu_B to account for this discrepancy. Redox anti-cooperativity occurs between redox centers and causes the midpoint potential of one centre to become lower when the other center is reduced (see [9] for a description of the redox anti-cooperativity between heme *a* and a_3). It often occurs due to electrostatic repulsion between reduced centers and is always reciprocal in nature so the lowering of the midpoint potential of one redox center due to the reduction of a second

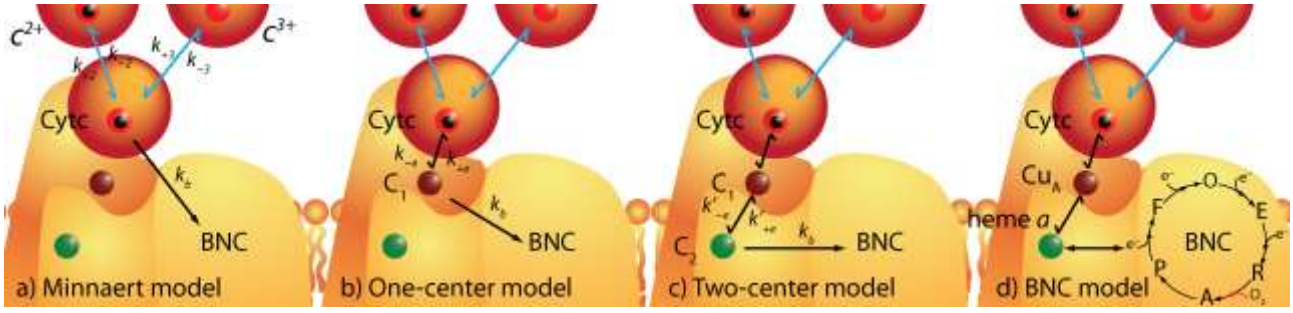

Figure 1. Graphical representations of the 4 models describing binding of Cyt*c* to CytOx and electron transfer. Both reduced Cyt*c* (c^{2+}) and oxidized Cyt*c* (c^{3+}) bind reversibly in all models. In the a) Minnaert model: bound reduced Cyt*c* is oxidized by the BNC in a single irreversible step. In the b) One-center model: the electron from reduced Cyt*c* is accepted reversibly by a single center (C_1) before being irreversibly oxidized by the BNC. In the c) Two-center model, the electron passes reversibly through two centers (C_1 and C_2) before being passed irreversibly to the BNC. Finally, in the d) BNC model, the electron is passed through the Cu_A and heme *a* centers before being passed to the BNC, which cycles through the 5 reductions states (P, F, O, E and R) before oxygen binding (A) and reduction of oxygen to regenerate (P). Blue bi-arrows depict reversible Cyt*c* binding and black bi-arrows/arrows denote reversible and irreversible electron transfers, respectively.

center is equal to the lowering of the midpoint potential of the second center due to reduction of the first. In the case of CytOx where the midpoint potential of Cu_A and heme *a* are similar, redox anti-cooperativity would make it more difficult to reduce both redox centers at low redox potentials so both would be more oxidized than would be predicted by a simple n=1 Nernst function, as observed experimentally. However, as low Cyt*c* redox potentials result in high turnover in the system studied, and any disequilibrium (deviation from equilibrium) is expected to be greater at high turnover, it is possible that the greater than expected oxidation at low redox potentials could be due to the loss of equilibrium between free Cyt*c* and bound Cyt*c* rather than redox anti-cooperativity.

Here we develop a more realistic model of Cyt*c* binding and electron transfer than the simple Minnaert model to explore the possible disequilibrium between free and bound Cyt*c*, and between bound Cyt*c* and the downstream redox centers. We first generate a model with a single redox center which accepts electrons from bound Cyt*c* and donates electrons to oxygen in an irreversible step (fig. 1b), that can be solved analytically. We then generate a second model with two redox centers downstream of Cyt*c* (fig. 2c) which is solved numerically. Finally, we develop a model in which electrons are transferred via Cu_A and heme *a* to the BNC which cycles through its 5 oxidation states (P, F, O, E and R) and binds and reduces molecular oxygen (fig. 1d).

Materials and Methods

The four models depicted in fig. 1 were solved in the steady state by assembling the chemical master equation of a state model. The Minnaert model has 3 states defined by the Cyt*c* binding site, which can be either empty (E), bound with reduced Cyt*c* (2) or bound with oxidized Cyt*c* (3).

$$\frac{d}{dt}\begin{pmatrix} E \\ 2 \\ 3 \end{pmatrix} = \begin{pmatrix} -k'_{+2}-k'_{+3} & k_{-2} & k_{-3} \\ k'_{+2} & -k_{-2}-k_b & 0 \\ k'_{+3} & k_b & -k_{-3} \end{pmatrix}\begin{pmatrix} E \\ 2 \\ 3 \end{pmatrix} \qquad \text{Equation 2}$$

$$k'_{+2} = k_{+2}[c^{2+}] \qquad k'_{+3} = k_{+3}[c^{3+}]$$

where k_{+2} and k_{-2} are the on and off rate constants for reduced (Fe^{2+}) Cyt*c*, k_{+3} and k_{-3} are likewise for oxidized (Fe^{3+}) Cyt*c*, $[c^{2+}]$ and $[c^{3+}]$ are the concentration of reduced and oxidized Cyt*c*, and k_b is the rate constant for oxidation of bound reduced Cyt*c*.

The one-center model has six states defined by the Cyt*c* binding site and the oxidation state of the redox center (O for oxidized, R for reduced). The chemical master equation is given by:

$$\frac{d}{dt}\begin{pmatrix} EO \\ 2O \\ 3O \\ ER \\ 2R \\ 3R \end{pmatrix} = \begin{pmatrix} -k'_{+2}-k'_{+3} & k_{-2} & k_{-3} & k_b & 0 & 0 \\ k'_{+2} & -k_{-2}-k_{+e} & 0 & 0 & k_b & k_{-e} \\ k'_{+3} & 0 & -k_{-3} & 0 & 0 & k_b \\ 0 & 0 & 0 & -k'_{+2}-k'_{+3}-k_b & k_{-2} & k_{-3} \\ 0 & 0 & 0 & k'_{+2} & -k_{-2}-k_b & 0 \\ 0 & k_{+e} & 0 & k'_{+3} & 0 & -k_{-3}-k_{-e}-k_b \end{pmatrix}\begin{pmatrix} EO \\ 2O \\ 3O \\ ER \\ 2R \\ 3R \end{pmatrix} \qquad \text{Equation 3}$$

where k_{+e} and k_{-e} are the forward and reverse rate constants for electron transfer from bound Cyt*c* to the redox center and here k_b is the rate constant for oxidation of the redox center. Finally, the two center model has 12 states, because the second redox center can also be oxidized or reduced, and the BNC model has 72 states as the BNC cycles through 6 states. The chemical master equation was then solved in the steady state by matrix inversion either analytically or numerically using a fixed total CytOx concentration.

The turnover data and oxidation states of Cu_A, heme *a* and the 655nm band were digitized from Mason et al. [6] which used 6.5μM of bovine CytOx and 10μM of horse Cyt*c* in 100mM potassium phosphate buffer with 0.1% lauryl maltoside at pH 7.4 and 30°C. The reductant was 40mM

ascorbate and Cyt*c* reduction state was varied by changing the concentration of N,N,N′,N′, tetramethyl-p-phenylenediamine (TMPD).

Results

The general solution of the Minnaert model is given by:

$$v_e = \frac{k_b k_{-3} k_{+2}[c^{2+}]}{(k_{-3}+k_b)k_{+2}[c^{2+}] + (k_{-2}+k_b)k_{+3}[c^{3+}] + k_{-3}(k_{-2}+k_b)} \qquad \text{Equation 4}$$

where v_e is the electron flux. This expression only follows Smith-Conrad kinetics if $k_{+2}=k_{+3}$ and $k_{-2}=k_{-3}$, that is, if the on rate constant (k_{on}) of reduced and oxidized Cyt*c* (k_{+2} and k_{+3}, respectively) are the same and likewise for the off rate constant (k_{off}) of reduced and oxidized Cyt*c* (k_{-2} and k_{-3}, respectively). This implies that the binding constants ($K_d=k_{off}/k_{on}$) of reduced and oxidized Cyt*c* are the same. Using this assumption, Van Buuren et al. [10] estimated that $k_{+2} = k_{+3} = 40\times10^6$ $M^{-1}s^{-1}$, $k_{-2} = k_{-3} = 1200$ s^{-1} and k_b =300 s^{-1} giving a k_{cat} of 240 s^{-1} and a K_d of 30μM.

In order to explore the effect of changing the relative K_d of oxidized and reduced Cyt*c*, which affects the midpoint potential of bound Cyt*c* (see supplementary information), we made the k_{on} for oxidized and reduced Cyt*c* the same but adjusted the k_{off} for oxidized and reduced Cyt*c* according to:

$$k_{-2} = 1200e^{-F\Delta E_{m,b}/2RT} \qquad \text{Equation 5}$$
$$k_{-3} = 1200e^{+F\Delta E_{m,b}/2RT}$$

where $\Delta E_{m,b}$ is the difference in midpoint potential between bound Cyt*c* and free Cyt*c* and the factor 1200 is the off rate determined by Van Buuren et al. Fig 2a compares the predicted turnover of the Minnaert model with the experimental data as the midpoint potential of bound Cyt*c* is changed according to eqn. 5. The model qualitatively matches the experimental data well when using 10μM of total *Cytc*, as per the experimental data, and the Van Buuren et al. values for the binding rate constants and k_b, (fig 2a) but the noise on the turnover data precludes using it to assess the midpoint

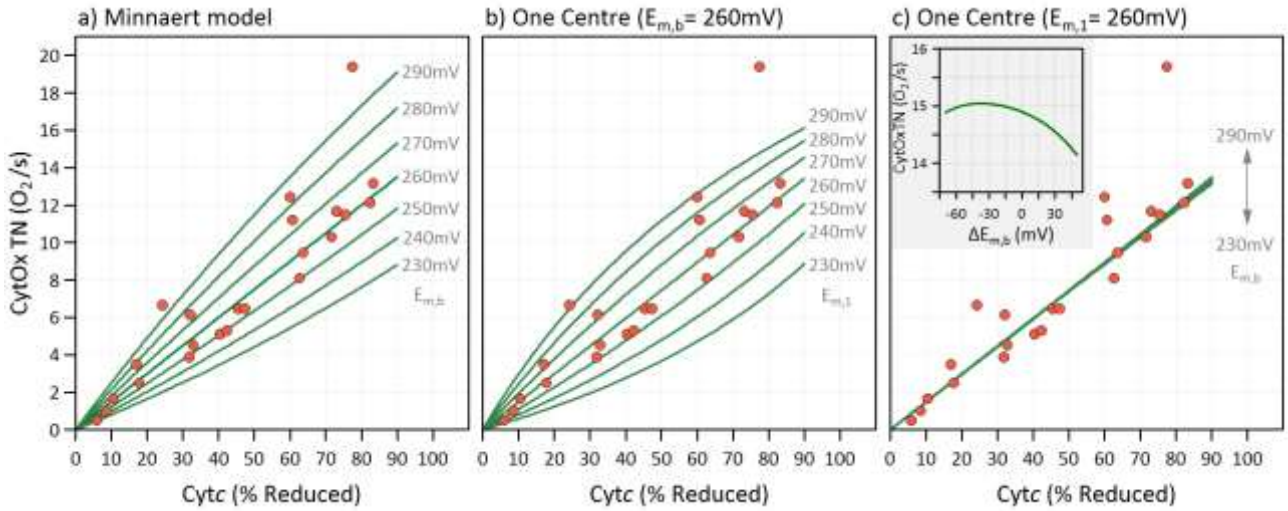

Figure 2. Comparison of experimental turnover data with the predicted by the Minnaert and the one-center model as the midpoint potential of either bound Cyt*c* ($E_{m,b}$) and the donating center ($E_{m,1}$) is varied. All models use 10μM of Cyt*c* as per the experimental data and a k_{-2} and k_{-3} of 40×10^6 M^{-1}. a) Minnaert model with k_b of 300 s^{-1} as the midpoint potential of bound Cyt*c* (E_m) is varied using eqn. 2. b) One-center model with k_b of 86 s^{-1}, keeping $E_{m,b}$ constant at 260mV and varying the midpoint potential of the donating center ($E_{m,1}$). c) as b) but keeping $E_{m,1}$ constant at 260mV and varying $E_{m,b}$. The insert shows the turnover as $E_{m,b}$ is varied when $E_{m,1}$ is held at 260mV with 10μM of reduced Cyt*c*.

potentials of the different centers. Instead, the condition that the enzyme must follow Conrad-Smith kinetics (linearity between turnover and Cyt*c* oxidation state at fixed Cyt*c* concentration) was used to determine their correct midpoint potentials. As expected, the model only precisely reproduces Smith-Conrad kinetics when the midpoint potential of the bound Cyt*c* is equal to the free Cyt*c* (260mV [6]), with the relationship between Cyt*c* and turnover becoming non-linear when the midpoint potentials are not equal (i.e. $k_{-2} \neq k_{-3}$). Furthermore, increasing the midpoint potential of bound Cyt*c* increases the k_{off} of oxidized Cyt*c* and so increases turnover, and vice versa.

The Minnaert model assumes that the bound reduced Cyt*c* is oxidized in an irreversible process. In reality, electrons are passed to Cu_A and heme *a* with forward and reverse rate constants that are large with respect to the net electron flux. This process was first modeled by extending the Minnaert model to include one center which accepts electrons from bound Cyt*c*, with reversible rate constants, and donates them to the BNC, with an irreversible rate constant of k_b (fig. 1b). The general solution for the one-center model is considerably more complex than the Minnaert model and given by:

$$v_e = \frac{k_{-3}k_{+e}k_b k_{+2}[c^{2+}]}{k_b A + k_{+e}k_b B + C\,A/D} \qquad \text{Equation 6}$$

$$A = k_{-3}k_{+2}[c^{2+}] + k_{-2}k_3[c^{3+}] + k_{-2}k_{-3}$$

$$B = k_{+2}[c^{2+}] + k_{+3}[c^{3+}] + k_{-3}$$

$$C = (k_{-3}k_{+e} + k_b k_{-e})k_{+2}[c^{2+}] + (k_{-2} + k_b)k_{-e}k_{+3}[c^{3+}] + (k_{-2} + k_b)k_{-e}k_b$$

$$D = A + k_b B + (k_{-2} + k_b)k_b$$

where k_{+e} and k_{-e} are the forward and reverse rate constants for electron transfer between bound and reduced Cyt*c* and the redox center. Similar to before, the midpoint potential of this center was varied by setting k_{+e}, k_{-e} to:

$$k_{+e} = 10^5 e^{+F(\Delta E_{m,1} - \Delta E_{m,b})/2RT} \qquad \text{Equation 7}$$

$$k_{-e} = 10^5 e^{-F(\Delta E_{m,1} - \Delta E_{m,b})/2RT}$$

where $\Delta E_{m,1}$ is the difference of the midpoint potential of the center and free Cyt*c*, and the factor 10^5 is the experimentally determined minimum rate for electron transfer from bound Cyt*c* to Cu_A [8]. The inclusion of $\Delta E_{m,b}$ ensures that the midpoint potential of the center is independent of the midpoint potential of bound Cyt*c* (see supplementary information). This model used the same Cyt*c* binding constants as the Minnaert model but, when using the same value for k_b, the turnover was much greater. This occurred because, although the donating center has the same oxidation state as the bound Cyt*c*, only a fraction of the binding sites are occupied by Cyt*c* and so the product of rate constant and concentration is smaller in the Minnaert model than in the one-center model. For this reason, the k_b used in the one-center model was decreased to 86 s^{-1}, so that the turnover numbers of the two models matched for a given Cyt*c* oxidation state. The dependency of this model on the midpoint potential of the donating center was then explored. For that, the binding rate constants for reduced and oxidized Cyt*c* were set the same values as in the Minnaert model (midpoint potential of bound Cyt*c* is equal to free Cyt*c*) and then the midpoint potential of the donating center was changed by varying the electron transfer rate constants according to eqn. 7 (fig 2b). As visible, the model reproduced Smith-Conrad kinetics when the donating center had the same midpoint potential as free Cyt*c* but showed a non-linear relationship between turnover and Cyt*c* when it differed (fig 2b).

To determine if the one-center model still required an equal k_{off} for both reduced and oxidized Cyt*c*, further simulations were carried out. We used the same k_{on} for reduced and oxidized Cyt*c*, fixed the midpoint potential of the donating center at 260mV and varied the midpoint potential of bound Cyt*c*

according to eqn. 5 and 7. Note this required changing the k_{off} of both reduced and oxidized Cyt*c* (eqn. 5) and the rate constants for electron transfer from bound Cyt*c* to the center (eqn. 7). These simulations showed that Conrad-Smith kinetics were maintained to within experimental accuracy regardless of the midpoint potential of bound Cyt*c*, as long as the donating center had the same midpoint potential as free Cyt*c* (fig. 2c).

As found with the Minnaert model, the turnover would be expected to be higher when the midpoint potential of bound Cyt*c* is higher and the k_{off} for oxidized Cyt*c* is greater. To examine this effect in more detail, simulations were carried out with 10 μM of reduced Cyt*c* and the turnover plotted as a function of the difference in midpoint potential between bound and free Cyt*c* (insert of fig. 2c). Surprisingly, the turnover was maximal when the midpoint potential of bound Cyt*c* was ≈ 35 to 40mV below that of free Cyt*c*, even though the k_{off} of oxidized Cyt*c* was smaller.

The condition that the donating center has the same midpoint potential as free Cyt*c* can be expressed as $k_{-3}k_{+e} = k_{-2}k_{-e}$ when the k_{on} for both oxidized and reduced Cyt*c* are the same. In addition, the term k_bA in the denominator of eqn. 6 is small compared to the other terms (k_b is much smaller than k_{+e} or k_{-e}) and so this term can be ignored. With these two conditions, eqn. 6 can be written as:

$$v_e = \frac{k_{-3}k_{+e}k_bk_{+2}[c^{2+}]}{\left(k_{+2}[c^{2+}]+k_{+3}[c^{3+}]\right)\left(k_{+e}k_b+\left(k_{-2}+k_b\right)k_{-e}\,A/D\right)+E} \qquad \text{Equation 8}$$

$$A = k_{-3}k_{+2}[c^{2+}]+k_{-2}k_{+3}[c^{3+}]+k_{-2}k_{-3}$$

$$D = A+k_b\left(k_{+2}[c^{2+}]+k_{+3}[c^{3+}]\right)+\left(k_{-2}+k_{-3}+k_b\right)k_b$$

$$E = k_{-3}k_{+e}k_b+\left(k_{-2}+k_b\right)k_{-e}k_b\,A/D$$

which approximates Smith-Conrad kinetics when $k_{+2}=k_{+3}$ because the term *A/D* is a very weak function of Cyt*c* oxidation state. From this we conclude that, to generate Smith-Conrad kinetics, (1) the k_{on} for oxidized and reduced Cyt*c* must be the same, (2) the k_{off} need not be the same and (3) the center which donates to oxygen must have the same midpoint potential as free Cyt*c*.

A two-center model was then used to explore the disequilibrium between free Cyt*c* and downstream redox centers. This model has two centers (C_1 and C_2, fig. 1c) in rapid equilibrium with bound Cyt*c* before a slow step to the BNC (fig. 1c). For these simulations, both the midpoint potential of bound Cyt*c* and that of C_2, which donates electrons to the BNC via a slow irreversible step, was fixed at 260mV to ensure Smith-Conrad kinetics. Then, the midpoint potential of C_1 was varied by changing the rate constants according to eqn. 7, and the midpoint potential of C_2 was fixed by varying the forward and reverse rate constant for electron transfer from centers C_1 to C_2 according to:

$$k'_{+e} = 10^5 e^{-F\Delta E_{m,1}/2RT} \qquad \text{Equation 9}$$

$$k'_{-e} = 10^5 e^{+F\Delta E_{m,1}/2RT}$$

where the term 10^5 reflects the rapid electron equilibration between Cu_A and heme *a* [11]. The turnover of this model displayed Smith-Conrad kinetics and varied very little with the midpoint potential of C_1 (fig. 3a). The redox potentials of the free Cyt*c* and of the two redox centers were calculated from their oxidation state (using an n=1 Nernst function) and their midpoint potentials. Then the ΔG for electron transfer from free Cyt*c* to C_1, and from C_1 to C_2, was determined from the differences in the above calculated redox potentials according to:

$$\Delta G = -\left(E_h^a - E_h^d\right) \qquad \text{Equation 10}$$

where $E_h{}^a$ and $E_h{}^d$ are the redox potentials of the accepting and donating centers, respectively. Fig 3b shows that, while there was a considerable disequilibrium between free Cyt*c* and C_1, which

increased with electron flux, both C_1 and C_2 remained in close equilibrium with a ΔG smaller than −2mV as the midpoint potential of bound Cyt*c* varied. These results are expected since, at a concentration of 10μM, the effective first order rate constant for Cyt*c* binding is only 400 s^{-1}, which is comparable to the 64 s^{-1} (4 times the CytOx turnover number) of the electron flux, whereas the rate constants for electron transfer between the centers are almost 3 orders of magnitude greater.

Fig. 3c compares the oxidation state of C_1 when it has different midpoint potentials to the experimentally measured oxidation state of the heme *a* center, Cu_A center and the 655nm band, which has been used as a surrogate of oxidized Cu_B [6]. As visible, the data suggests that these centers have midpoint potentials of ≈280, ≈250 and ≈260mV, respectively. Also, there is very good correspondence between the model and the data except when Cyt*c* is more than 80% reduced, where the model substantially underestimates the reduction of the 655nm band and slightly underestimates the reduction of heme *a*. This data strongly suggests that the non Nernst response of Cu_A and heme *a* centers could result from the disequilibrium between free Cyt*c* and Cu_A rather than from redox anti-cooperativity.

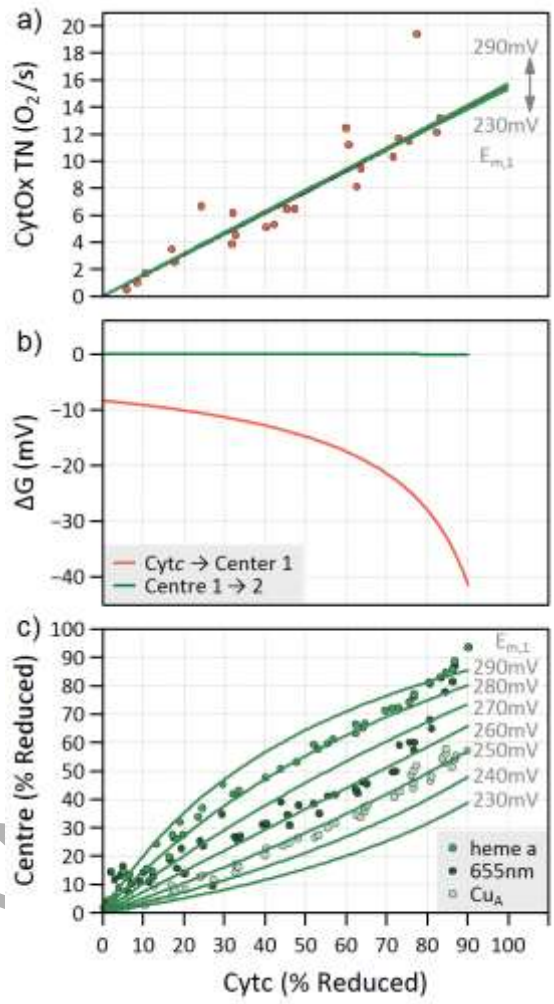

Figure 3. Disequilibrium between free Cyt*c* and the redox centers (C_1 and C_2) in a two-center model, in which the midpoint potentials of both bound Cyt*c* and of C_2 were held at 260mV. a) Comparison of experimental (circles) and modelled turnover data as the midpoint potential of the C_1 is varied. b) Modelled disequilibrium between free Cyt*c* and C_1, and between C_1 and C_2, when C_1 and C_2 have a midpoint potential of 260mV. c) Comparison of the experimental oxidation states of Cu_A, heme *a* and the 655nm band (circles) with the modelled oxidation state of C_1 when the midpoint potential of the center is varied between 230 and 290mV (lines).

The redox chemistry at the BNC is considerably more complex than assumed in the previous models (see [12] for a review). The BNC cycles though the states P, F, O, E and R with each transition requiring an electron from heme *a* and a substrate proton from the matrix. The state P has Cu_B oxidized, heme a_3 in the ferryl (Fe^{4+}) form and a nearby tyrosine as a free radical. The first electron reduces the tyrosine to generate state F and the second electron reduces heme a_3 to the ferric (Fe^{3+}) form to generate the state O. State O can relax into a slow form in which further electron transfer to the BNC is very slow and not thought to be part of the catalytic cycle [13]. Alternatively, the third electron reduces Cu_B to form state E and the fourth electron reduces heme a_3 to form state R. Molecular oxygen binds to state R to form state A whereupon the oxygen undergoes a concerted and irreversible 4-electron reduction to regenerate state P.

The midpoint potentials of the P/F and F/O couples are very high (≈800mV) [14-15] making these transitions essentially irreversible. Heme *a* and the BNC are sufficiently close that electron transfers occur on the nanosecond timescale [16]. However, the reduction of the BNC from P to F and from F to O are much slower than the pure electron transfers because these transitions also involve proton pumping and proton uptake to the BNC which determine the equilibrium. Nonetheless, these transitions are rapid with respect to turnover and state P is reduced to state F and O with time constants of 0.2 and 3ms after oxygen reduction when both Cu_A and heme *a* are initially reduced [17]. Likewise the binding and reduction of oxygen is also very rapid with rate constants of 1.38×10^8 $M^{-1}s^{-1}$ (2.76×10^4 at 200μM of oxygen) and 0.32×10^5 s^{-1}, respectively [18]. During

turnover, heme a_3 is observed to be highly oxidized. This can easily be explained if either the O/E or E/R transition is slow compared to oxygen binding and reduction such that heme a_3 is oxidized much faster than it is reduced. When reduced Cyt*c* and oxidized CytOx are mixed in a stop flow experiment, there is an initial burst phase in which Cu_A and heme *a* are reduced that is then followed by a slow phase of Cyt*c* oxidation with a rate 51 s^{-1} that does not have spectral signal, consistent with the reduction of Cu_B [19]. This would suggest that the O/E transition is slow.

Using these observations, a model was developed in which the BNC cycled through states P to R on transfer of an electron from heme *a*, and then spontaneously to state A before regenerating P (fig. 1d). The model used the same rate constants for Cyt*c* binding as the Minnaert model and the same rate constants for electron transfer from bound Cyt*c* to Cu_A and heme *a* with the latter centers having a midpoint potential of 280 and 245mV, respectively. The forward rate constants for the P/F and F/O transitions were set to 5.0×10^4 and 3.33×10^2 s^{-1}, respectively, consistent with the experimental results [17], and the reverse rates constants were essentially zero due to the large ΔG^0 of the electron transfer. The reverse rate constant of the E/R transition had no effect on turnover because the rapid binding and reduction of oxygen reduces the probability of finding the enzyme in the R state to near zero. The forward rate constant and midpoint potential of the O/E transition and the forward rate constant of the E/R transition was then tuned by trial and error. The best correspondence between experimental and modeled data was found when Cu_B had a midpoint potential of 260mV and the forward rate constants for the O/E and E/R transitions were 200 and 30 s^{-1}, respectively (fig. 4). With these parameters

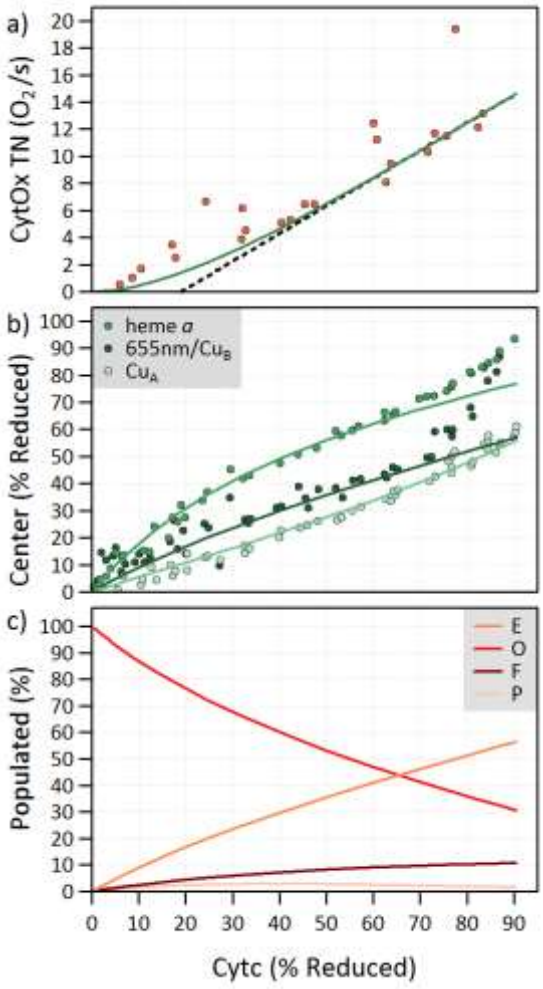

Figure 4. Comparison of experimental data with that predicted by the BNC model. a) Experimental (circles) and modelled (solid line) turnover data. The dotted line is a regression to the linear component of the modelled turnover. b) Experimental oxidation states of Cu_A, heme *a* and the 655nm band (circles) compared to modelled oxidation state of Cu_A, heme *a* and Cu_B (lines). c) Modelled population of states P, F, O and E during turnover.

Table 1 Reactions, rate constants and standard free energies of the BNC model.

Reaction	BNC	k_f	k_r	ΔG^0 *(mV)*
PB Cytc^{2+}		40.0×10^6 [C^{2+}]	1.2×10^3	−278
PB Cytc^{3+}		40.0×10^6 [C^{3+}]	1.2×10^3	−278
ET Cyt*c* → Cu_A		100×10^3	175×10^3	15
ET Cu_A → heme *a*		100×10^3	27.0×10^3	−35
ET heme *a* → BNC	(P→F)	5×10^3	1.74×10^{-5}	−520
ET heme *a* → BNC	(F→O)	3.33×10^2	1.16×10^{-6}	−520
ET heme *a* → BNC	(O→E)	200	423	20
ET heme *a* → BNC	(E→R)	30	63.4†	20†
MB O_2 → BNC	(R→A)	$1.38\times10^8[O_2]$	38.6×10^3	−220
OR	(A→P)	6.67×10^3	0.01	−360

Key: PB: protein binding, ET: electron transfer, MB molecular binding, OR: oxygen reduction. † The turnover of the model has negligible dependency on these values because the R state population is near zero. The square brackets denote concentration in Molar.

(summarized in table 1), the model produced Conrad-Smith kinetics when Cyt*c* was more than ≈40% reduced (fig 4a), and there was a good correspondence between the modeled and experimental oxidation states of Cu_A and heme *a* and between Cu_B and the 655nm band (fig 4b). Furthermore, the model predicted that CytOx population of the P and F states were below 10% (fig. 4c) and negligible reduction of heme a_3, both consistent with experimental observations [6].

Discussion

In this paper we have taken the Minnaert model and added additional complexity to arrive at a very simple but more realistic model of CytOx turnover that can account for the non Nernst response of Cu_A and heme *a* and gives a good approximation to Smith-Conrad kinetics. The model predicts that the effective midpoint potential of Cu_A and heme *a* are ≈245 and ≈280mV, respectively, the former in good agreement with redox titrations (250mV) [7] and the latter in good agreement with calculations from time resolved studies at short timescales (270mV) [11, 20] but markedly different from 340mV recorded for heme *a* when heme a_3 is oxidized in long-timescale redox titrations [21]. This work finds that the non Nernst response of Cu_A and heme *a* is most likely due to the disequilibrium between free Cyt*c* and Cu_A, as result of the relatively slow kinetics of Cyt*c* binding and release compared to turnover, rather than redox anti-cooperativity. While the Minnaert model requires the k_{off} to be the same for both reduced and oxidized Cyt*c* to reproduce Smith-Conrad kinetics, the more realistic models find this is not necessary. Our model including the BNC predicts low populations of CytOx in the P, F and R states during turnover, as found experimentally [6]. Overall, this work paints a picture in which the transfer of electrons from the pool of free Cyt*c* to Cu_A is relatively slow (τ≈2.5ms), due to the slow binding and release of Cyt*c*, the equilibration of electrons between bound Cyt*c*, Cu_A and heme *a* is fast (τ≈8μs) whereas the transfer of electrons to oxygen is, again, slow. The electron transfer to the BNC is fastest in states F and P (τ≈0.2 and 3ms, respectively), relatively slow transfer in the state O (τ≈5ms) and slowest in state E (τ≈30ms), when electron transfer reduces heme a_3.

The simplest way to determine if the non-Nernst response between Cytc, Cu_A, heme *a* and the 655nm band is due to redox anti-cooperativity or redox disequilibrium would be to repeat the studies with varying concentrations of Cyt*c*. If there is close equilibrium between free Cyt*c* and Cu_A and the non-Nernst response is due to redox anti-cooperativity then the response should not change with Cyt*c* concentration. In contrast, if the response is due to disequilibrium between Cyt*c* and Cu_A then the disequilibrium should become greater at low Cyt*c* concentrations.

The 655nm absorption band is thought to originate from a charge transfer band from oxidized heme a_3 and a bound ligand that is only present when Cu_B is oxidized [22]. Therefore, it is expected to appear when the BNC is in the state O but not the state E and, as such, it has been used previously by others as a surrogate of oxidized Cu_B [6]. The band titrates with a midpoint potential of ≈400mV in redox titrations [22] and would be expected to have a midpoint potential >460mV from the time resolved O to E transition [11]. Here the band has a good correlation with Cu_B when it has a midpoint potential of 260mV. Surprisingly, this value is needed by the donating center in the simpler models to produce Smith-Conrad kinetics even though electrons are donated to the BNC by heme *a* and not Cu_B. It is known that the state O is metastable [13] and can relax into a slow form which cannot pump protons and in which Cu_B has a low midpoint potential reminiscent of the form found here [23]. However, the low apparent midpoint potential of Cu_B cannot be attributed to the relaxation of state O under the conditions modeled here because the lifetime of O is at least 30 seconds [13] whereas the enzyme is turning over on a much shorter timescale. The reason why Cu_B has such an apparent low midpoint potential is not known but raising the midpoint potential in the model led to larger deviations from Smith-Conrad kinetics and a substantial mismatch between the 655nm band and the oxidation state of Cu_B.

Based on the Dutton ruler [24], the intrinsic electron transfer rate from heme *a* to the BNC is expected to be on the nanosecond timescale due to their proximity [16], whereas the model uses rate

constants on the millisecond timescale. This disparity is thought to occur because electron transfer is coupled to protonation and the proton uptake is slow. In state O, prior to proton uptake, the midpoint potential of heme *a* is ≈270mV and that of the BNC is very low (<140mV) so that the equilibrium prevents electron transfer [11]. Uptake of the pump proton (τ≈0.15ms) raises the midpoint potential of heme *a* and the BNC via an electrostatic interaction to values approximating those seen in steady state redox transitions (≈340mV), altering the equilibrium so that the electron can be shared between heme *a* and the BNC. Subsequently, the substrate proton is taken up (τ≈0.8ms) and reacts with the oxygen intermediates at the BNC raising the midpoint potential of Cu_B to >460mV [11]. Technical limitations prevent such detailed studies on the E to R transition, but it could be expected that the pump proton raises the midpoint potential of heme *a* and a_3 similarly to the O to E transition, because it occurs through similar electrostatic interactions. In contrast the substrate proton undergoes different chemistry at the BNC and so will have a different effect on the midpoint potential of heme a_3 compared to Cu_B. The F to P and P to O transitions will be different again because heme a_3 is in the ferryl state instead of the ferric state and electron transfer has been found to occur before uptake of the pump proton [25]. However, the slow electron transfer to the state O seen here (τ≈5ms) is still slow compared to the uptake of the pump proton (τ≈0.15ms) and the substrate proton (τ≈0.8ms) in the time resolved studies. A similar discrepancy has been observed for the release of a proton during back flow studies on the R to E transition and has been attributed to different proton kinetics in the soluble enzyme modeled here compared to the time resolved studies carried out with the enzyme inserted into a membrane [26]. During catalytic turnover, the probability of finding the enzyme in states O and E is ≈90% (fig. 4c). In these states, heme *a* is expected to have midpoint potentials of ≈270mV, prior to pump proton uptake, and ≈340mV after proton uptake. The observed heme *a* midpoint potential of ≈280mV would suggest that the rate limiting step is the pump proton uptake rather than the substrate proton.

Transferring electrons from free Cyt*c* into CytOx with a small ΔG is a challenge. Electron transfer between Cyt*c*, Cu_A and heme *a* is much faster than the off rate for Cyt*c*, therefore the electron will equilibrate between these three centers in the time that Cyt*c* remains bound. Assuming midpoint potentials of 260, 250 and 280mV for Cyt*c*, Cu_A and heme *a*, respectively, the equilibrium will distribute one electron over the three redox centers at a proportion of 26:18:56%, respectively. In this case, Cyt*c* will leave the docking site reduced in 26% of docking events and only 74% of the events will result in electron transfer. If the three centers do not reach equilibrium before release of Cyt*c* then even fewer binding events will result in electron transfer. The situation is worse for the second electron because the equilibrium is 66:50:84 for two electrons over the three redox centers and so only 34% of dockings events will lead to electron transfer. This means that the burst phase of Cu_A and heme *a* reduction in time resolved studies [19-20, 27-28] must involve multiple dockings, and net electron transfer occurs with decreasing efficiency until there is equilibration of the redox potentials of the free Cyt*c*, Cu_A and heme *a* [27]. The electron transfer efficiency of a docking can be increased if oxidized Cyt*c* binds tighter to CytOx lowering the midpoint potential of the bound Cyt*c*. For instance, lowering the midpoint potential by 30mV would increase the electron transfer efficiency to 90% and 61% for the first and second electron, respectively. Equal affinity for reduced and oxidized Cyt*c* is a condition for the Minnaert model to generate Smith-Conrad kinetics, but we show this condition is relaxed in more realistic models. The k_{on} of reduced and oxidized Cyt*c* must be the same to generate Smith-Conrad kinetics (the term $k_{+2}[c^{2+}]+k_{+3}[c^{3+}]$ appearing in the rate equation must be independent of oxidation state), but the k_{off} and K_d can be different, as found when the K_d was measured directly [29]. When the midpoint potential of bound Cyt*c* is lower than free Cytc, the increase in electron transfer efficiency comes at the expense of a decreased k_{off} of oxidized Cyt*c* and, although maximum turnover occurred in the one-center model when the bound Cyt*c* had a midpoint potential 40mV lower than free Cyt*c* (inset of fig 2c), the increase in turnover was marginal (1%). Nevertheless, this work shows that k_{off} cannot be assumed to be the same for oxidized and reduced Cyt*c* in the burst phase of time resolved models.

The Cyt*c* concentration in the intermembrane space of mitochondria in living cells (≈700μM [30]) is much higher than that used here (10μM) and, consequently, the apparent first order k_{on} (k'_{+2} and k'_{+3} of eqn. 2) will be much higher than modeled here (28000s^{-1} compared to 400s^{-1}). This will bring the Cu_A center closer to equilibrium with the free Cyt*c* for a given turnover number under these conditions and the k_{off} will become the limiting factor in maintaining equilibrium between bound and free Cyt*c*. The k_{off} is equal to the product of k_{on} and the K_d so that the K_d becomes an important parameter when understanding the function *in-vivo*. The Minnaert model provides a simple framework to calculate K_d from experimental data because it predicts that the K_d is equal to the K_M [31]. However, this relationship is not maintained in the more realistic models where the K_M (3.48μM, 2.85μM and 3.56μM for the one-center, two-center and BNC model, respectively) was found to be an order of magnitude smaller than the K_d of the model (30μM). The K_d has also been estimated from time resolved studies where either reduced Cyt*c* and CytOx are rapidly mixed in a stopped-flow apparatus [20] or the free Cyt*c* is rapidly photo-reduced in a pre-mixed solution [19, 28]. The stopped-flow study found that the binding rates were strongly dependent on the ionic strength, suggesting that electrostatic interactions funnel the positively charged Cyt*c* towards the negatively charged binding site on CytOx [32], but the K_d was independent of ionic strength consistent with binding occurring mainly through hydrophobic interactions [31]. The K_d was found to be 1-2μM in the stopped-flow study and ≈10-13μM in the photo-reduction studies. All the studies required the use of a model to calculate k_{on} and K_d from the experimental data. The stopped-flow measurements were calculated with a model in which Cyt*c* binding was slow but electron transfer was very fast, consistent with later direct measurements of electron transfer rates from bound Cyt*c* to Cu_A and heme *a* [8]. In contrast, the photo-reduction studies used a model in which Cyt*c* binding was very fast but electron transfer from bound Cyt*c* was very slow, placing a question mark on the accuracy of the calculated K_d. Where the K_d was measured directly from the bound and free concentrations of Cyt*c* [29], it was found to be even lower at 0.35 and 0.13μM for reduced and oxidized Cyt*c*, respectively. Thus the different methodologies have produced values for K_d varying over two orders of magnitude from 0.13μM to 30μM with the higher values being calculated using questionable models. If the K_d is as low as 1μM, or even lower, then the k_{on} must be an order of magnitude greater than used here to support a k_{cat} of 25 O_2/s.

Acknowledgements

This research did not receive any specific grant from funding agencies in the public, commercial, or not-for-profit sectors.

References

1. S. Shimada, K. Shinzawa-Itoh, J. Baba, S. Aoe, A. Shimada, E. Yamashita, J. Kang, M. Tateno, S. Yoshikawa, and T. Tsukihara, *Complex structure of cytochrome c-cytochrome c oxidase reveals a novel protein-protein interaction mode.* EMBO J, 2017. 36(3): p. 291-300.

2. H. Conrad and L. Smith, *A study of the kinetics of the oxidation of cytochrome c by cytochrome c oxidase.* Arch Biochem Biophys, 1956. 63(2): p. 403-13.

3. L. Michaelis and M.L. Menten, *Die Kinetik der Invertinwirkung.* Biochem. Z., 1913. 49: p. 333-69.

4. A. Cornish-Bowden, J.P. Mazat, and S. Nicolas, *Victor Henri: 111 years of his equation.* Biochimie, 2014. 107 Pt B: p. 161-6.

5. K. Minnaert, *The kinetics of cytochrome c oxidase. I. The system: cytochrome c-cytochrome oxidase-oxygen.* Biochim Biophys Acta, 1961. 50: p. 23-34.

6. M.G. Mason, P. Nicholls, and C.E. Cooper, *The steady-state mechanism of cytochrome c oxidase: redox interactions between metal centres.* Biochem J, 2009. 422(2): p. 237-46.

7. E.A. Gorbikova, K. Vuorilehto, M. Wikstrom, and M.I. Verkhovsky, *Redox titration of all electron carriers of cytochrome c oxidase by Fourier transform infrared spectroscopy.* Biochemistry, 2006. 45(17): p. 5641-9.

8. L.P. Pan, S. Hibdon, R.Q. Liu, B. Durham, and F. Millett, *Intracomplex electron transfer between ruthenium-cytochrome c derivatives and cytochrome c oxidase.* Biochemistry, 1993. 32(33): p. 8492-8.

9. R.W. Hendler and H.V. Westerhoff, *Redox interactions in cytochrome c oxidase: from the "neoclassical" toward "modern" models.* Biophys J, 1992. 63(6): p. 1586-604.

10. K.J. van Buuren, B.F. van Gelder, and T.A. Eggelte, *Biochemical and biophysical studies on cytochrome aa 3 . I. Steady-state kinetics of cytochrome aa 3.* Biochim Biophys Acta, 1971. 234(3): p. 468-80.

11. I. Belevich, D.A. Bloch, N. Belevich, M. Wikstrom, and M.I. Verkhovsky, *Exploring the proton pump mechanism of cytochrome c oxidase in real time.* Proc Natl Acad Sci U S A, 2007. 104(8): p. 2685-90.

12. I. Belevich and M.I. Verkhovsky, *Molecular mechanism of proton translocation by cytochrome c oxidase.* Antioxid Redox Signal, 2008. 10(1): p. 1-29.

13. D. Bloch, I. Belevich, A. Jasaitis, C. Ribacka, A. Puustinen, M.I. Verkhovsky, and M. Wikstrom, *The catalytic cycle of cytochrome c oxidase is not the sum of its two halves.* Proc Natl Acad Sci U S A, 2004. 101(2): p. 529-33.

14. G.T. Babcock and M. Wikstrom, *Oxygen activation and the conservation of energy in cell respiration.* Nature, 1992. 356(6367): p. 301-9.

15. M. Wikstrom, K. Krab, and V. Sharma, *Oxygen Activation and Energy Conservation by Cytochrome c Oxidase.* Chem Rev, 2018. 118(5): p. 2469-2490.

16. M.I. Verkhovsky, A. Jasaitis, and M. Wikstrom, *Ultrafast haem-haem electron transfer in cytochrome c oxidase.* Biochim Biophys Acta, 2001. 1506(3): p. 143-6.

17. K. Faxen, G. Gilderson, P. Adelroth, and P. Brzezinski, *A mechanistic principle for proton pumping by cytochrome c oxidase.* Nature, 2005. 437(7056): p. 286-9.

18. M.I. Verkhovsky, J.E. Morgan, and M. Wikstrom, *Oxygen binding and activation: early steps in the reaction of oxygen with cytochrome c oxidase.* Biochemistry, 1994. 33(10): p. 3079-86.

19. J.T. Hazzard, S.Y. Rong, and G. Tollin, *Ionic strength dependence of the kinetics of electron transfer from bovine mitochondrial cytochrome c to bovine cytochrome c oxidase.* Biochemistry, 1991. 30(1): p. 213-22.

20. T.M. Antalis and G. Palmer, *Kinetic characterization of the interaction between cytochrome oxidase and cytochrome c.* J Biol Chem, 1982. 257(11): p. 6194-206.

21. N. Kojima and G. Palmer, *Further characterization of the potentiometric behavior of cytochrome oxidase. Cytochrome alpha stays low spin during oxidation and reduction.* J Biol Chem, 1983. 258(24): p. 14908-13.

22. R. Mitchell, P. Mitchell, and P.R. Rich, *The assignment of the 655 nm spectral band of cytochrome oxidase.* FEBS Lett, 1991. 280(2): p. 321-4.

23. V. Sharma, K.D. Karlin, and M. Wikstrom, *Computational study of the activated O(H) state in the catalytic mechanism of cytochrome c oxidase.* Proc Natl Acad Sci U S A, 2013. 110(42): p. 16844-9.

24. C.C. Moser, T.A. Farid, S.E. Chobot, and P.L. Dutton, *Electron tunneling chains of mitochondria.* Biochim Biophys Acta, 2006. 1757(9-10): p. 1096-109.

25. A. Namslauer, A. Aagaard, A. Katsonouri, and P. Brzezinski, *Intramolecular proton-transfer reactions in a membrane-bound proton pump: the effect of pH on the peroxy to ferryl transition in cytochrome c oxidase.* Biochemistry, 2003. 42(6): p. 1488-98.

26. I. Belevich, A. Tuukkanen, M. Wikstrom, and M.I. Verkhovsky, *Proton-coupled electron equilibrium in soluble and membrane-bound cytochrome c oxidase from Paracoccus denitrificans.* Biochemistry, 2006. 45(12): p. 4000-6.

27. L.E. Andreasson, *Characterization of the reaction between ferrocytochrome c and cytochrome c oxidase.* Eur J Biochem, 1975. 53(2): p. 591-7.

28. R.W. Larsen, J.R. Winkler, and S.I. Chan, *Photoinitiated Electron-Transfer between Cytochrome-C and Cytochrome-C-Oxidase Using a Novel Uroporphyrin Nadh Reducing System.* Journal of Physical Chemistry, 1992. 96(20): p. 8023-8027.

29. L.C. Petersen, *Cytochrome c--cytochrome aa3 complex formation at low ionic strength studied by aqueous two-phase partition.* FEBS Lett, 1978. 94(1): p. 105-8.

30. M.O. Ripple, M. Abajian, and R. Springett, *Cytochrome c is rapidly reduced in the cytosol after mitochondrial outer membrane permeabilization.* Apoptosis, 2010. 15(5): p. 563-73.

31. W. Sato, S. Hitaoka, K. Inoue, M. Imai, T. Saio, T. Uchida, K. Shinzawa-Itoh, S. Yoshikawa, K. Yoshizawa, and K. Ishimori, *Energetic Mechanism of Cytochrome c-Cytochrome c Oxidase Electron Transfer Complex Formation under Turnover Conditions Revealed by Mutational Effects and Docking Simulation.* J Biol Chem, 2016. 291(29): p. 15320-31.

32. G. Schreiber and A.R. Fersht, *Rapid, electrostatically assisted association of proteins.* Nat Struct Biol, 1996. 3(5): p. 427-31.

Figure Captions

Figure 1. Graphical representations of the 4 models describing binding of Cyt*c* to CytOX and electron transfer. Both reduced Cyt*c* (c^{2+}) and oxidized Cyt*c* (c^{3+}) bind reversibly in all models. In the a) Minnaert model: bound reduced Cyt*c* is oxidized by the BNC in a single irreversible step. In the b) One-center model: the electron from reduced Cyt*c* is accepted reversibly by a single center (C_1) before being irreversibly oxidized by the BNC. In the c) Two-center model, the electron passes reversibly through two centers (C_1 and C_2) before being passed irreversibly to the BNC. Finally, in the d) BNC model, the electron is passed through the Cu_A and heme *a* centers before being passed to the BNC, which cycles through the 5 reductions states (P, F, O, E and R) before oxygen binding (A) and reduction of oxygen to regenerate (P). Blue bi-arrows depict reversible Cyt*c* binding and black bi-arrows/arrows denote reversible and irreversible electron transfers, respectively.

Figure 2. Comparison of experimental turnover data with the predicted by the Minnaert and the one-center model as the midpoint potential of either bound Cyt*c* ($E_{m,b}$) and the donating center ($E_{m,1}$) is varied. All models use 10μM of Cyt*c* as per the experimental data and a k_{-2} and k_{-3} of 40×10^6 M^{-1}. a) Minnaert model with k_b of 300 s^{-1} as the midpoint potential of bound Cyt*c* (E_m) is varied using eqn. 3. b) One-center model with k_b of 86 s^{-1}, keeping $E_{m,b}$ constant at 260mV and varying the midpoint potential of the donating center ($E_{m,1}$). c) as b) but keeping $E_{m,1}$ constant at 260mV and varying $E_{m,b}$. The insert shows the turnover as $E_{m,b}$ is varied when $E_{m,1}$ is held at 260mV with 10μM of reduced Cyt*c*.

Figure 3. Disequilibrium between free Cytc and the redox centers (C1 and C2) in a two-center model, in which the midpoint potentials of both bound Cytc and of C2 were held at 260mV. a) Comparison of experimental (circles) and modelled turnover data as the midpoint potential of the C1 is varied. b) Modelled disequilibrium between free Cytc and C1, and between C1 and C2, when

C1 and C2 have a midpoint potential of 260mV. c) Comparison of the experimental oxidation states of CuA, heme a and the 655nm band (circles) with the modelled oxidation state of C1 when the midpoint potential of the center is varied between 230 and 290mV (lines).

Figure 4. Comparison of experimental data with that predicted by the BNC model. a) Experimental (circles) and modelled (solid line) turnover data. The dotted line is a regression to the linear component of the modelled turnover. b) Experimental oxidation states of CuA, heme a and the 655nm band (circles) compared to modelled oxidation state of CuA, heme a and CuB (lines). c) Modelled population of states P, F, O and E during turnover.

Graphical Abstract